

Modal Analysis of Lightweight Graphite Reinforced Silica/Polymer Matrix Composite Plates

by T.K. Ooi, J.A. Gilbert, M.V. Bower, R.E. Vaughan and R.C. Engberg

ABSTRACT—In this paper we describe how finite element and experimental modal analyses can be used to characterize the dynamic behavior of plates made from a new class of graphite reinforced silica/polymer matrix composite (GRSPMC) materials. An agreement is obtained between both methods, and the results show that GRSPMC materials can be modeled and tested using tools similar to those applied to the study of classical composite laminates.

KEY WORDS—Composite materials, cementitious composites, modal analysis, structural testing, finite element modeling

Introduction

A limited number of static tests have been performed to determine the material properties of graphite reinforced silica/polymer matrix composites (GRSPMCs).^{1,2} In this paper we describe how finite element and experimental modal analyses can be used to characterize the dynamic behavior of plates made from these materials. The results will help researchers to predict the dynamic response of large structures fabricated from these composites.

During this study, finite element models were developed based on classical laminated plate theory. In the experimental investigations, we began by studying five plates having the same aspect ratio in order to determine how the uncertainties in the material properties, due to a large number of variables associated with the fabrication process, affected modal parameters. Then, plates with aspect ratios ranging from 0.5 to 4.5 were impact tested in a free-hanging configuration to determine their natural frequencies and mode shapes.

The test results were compared to those obtained from finite element analyses to validate the finite element models. Results show that GRSPMC materials can be modeled and tested using tools similar to those applied to the study of classical composite laminates.

GRSPMC Plate Fabrication

A large 81.30 × 142.20 cm² GRSPMC plate was fabricated by placing the silica/polymer mixture described in

Dr. T.K. Ooi is a (TITLE), Dr. J.A. Gilbert (jag@eng.uah.edu) is a (TITLE) and Dr. M.V. Bower is a (TITLE), Department of Mechanical and Aerospace Engineering, University of Alabama in Huntsville, Huntsville, AL, USA. Dr. R.E. Vaughan is a (TITLE), Aviation Engineering Directorate, Structures and Materials Division, Redstone Arsenal, AL, USA. Mr. R.C. Engberg is a (TITLE), National Aeronautics and Space Administration (NASA) Marshall Space Flight Center, AL, USA.

Original manuscript submitted: 18 November, 2003.

Final manuscript received: 24 January, 2005.

DOI: 10.1177/0014485105053800

Table 1 over three layers of graphite reinforcement. Test plates having different aspect ratios were later cut from this plate.

According to the manufacturer, each layer of reinforcement consists of a non-impregnated graphite mesh with 3000 fibers per tow, spaced at 3.18 mm intervals. Each tow is 0.19 mm thick by 1.07 mm wide; the elastic modulus and tensile strength of the graphite are 231 and 3.65 GPa, respectively.

The mixture was prepared by first mixing the silica and microbubbles. Then the acrylic fortifier, latex, and water were added to produce a mixture having a smooth texture. The plate was fabricated by placing the first layer of graphite reinforcement [90°, 90°] on top of a plexi-glass sheet. Wires having a thickness of 2.54 mm were affixed at 7.62 cm intervals over the mesh and the mixture was placed over this configuration. After 12 h, the wires were removed and the grooves filled with the mixture. This process was repeated for the remaining layers, while we made sure not to place wires over the same locations used while constructing the previous layer. After letting the plate cure for seven days, it was cut into smaller plates having different aspect ratios.

GRSPMC Laminate Constitutive Equations

The constitutive equations that relate the force and moment resultants to the strains for GRSPMC anisotropic plates can be derived based on the classical laminated plate theory and may be written as^{3,4}

$$\begin{bmatrix} N_x \\ N_y \\ N_{xy} \\ M_x \\ M_y \\ M_{xy} \end{bmatrix} = \begin{bmatrix} A_{11} & A_{12} & A_{13} & B_{11} & B_{12} & B_{13} \\ A_{21} & A_{22} & A_{23} & B_{21} & B_{22} & B_{23} \\ A_{31} & A_{32} & A_{33} & B_{31} & B_{32} & B_{33} \\ B_{11} & B_{12} & B_{13} & D_{11} & D_{12} & D_{13} \\ B_{21} & B_{22} & B_{23} & D_{21} & D_{22} & D_{23} \\ B_{31} & B_{32} & B_{33} & D_{31} & D_{32} & D_{33} \end{bmatrix} \begin{bmatrix} \varepsilon_{0x} \\ \varepsilon_{0y} \\ \gamma_{0xy} \\ K_x \\ K_y \\ K_{xy} \end{bmatrix} \quad (1)$$

where

$$(A_{ij}, B_{ij}, D_{ij}) = \sum_{r=1}^N \int_{z_r}^{z_{r+1}} Q_{ij}^{(r)}(1, z, z^2) dz.$$

TABLE 1—MIX PROPORTIONS

Ingredient	% Mass (weight)
K-25 Glass bubbles	11.75
Portland cement	30.06
Latex	16.70
Acrylic fortifier	8.08
Water	33.41

Here, N_x , N_y , and N_{xy} are the resultant force and shear force in the x -axis, y -axis, and $x - y$ -plane, respectively; M_x , M_y , and M_{xy} are the resultant moment and twisting about the x -axis, y -axis, and $x - y$ -plane, respectively; Z_r and Z_{r+1} are the thickness coordinates of the lower and upper surfaces of the r th ply, respectively; $Q_{ij}^{(r)}$ is the material stiffness of the r th ply; Z is the laminate transverse direction, normal to the $x - y$ -plane; N is the number of plies in the laminate; ϵ_{0x} , ϵ_{0y} , and γ_{0xy} are the mid-plane strains in the x -axis, y -axis, and $x - y$ -plane, respectively; K_x , K_y , and K_{xy} are the plate bending curvatures in the $x - z$ -plane, $y - z$ -plane, and $x - y$ -plane, respectively; A_{ij} is the extensional stiffness; B_{ij} is the bending-extension coupling stiffness; and D_{ij} is the bending stiffness.

The A , B , and D matrices are computed based on the laminate material properties, geometry, and stacking sequence. For a three-ply specially orthotropic laminate (a laminate whose principal material axes are aligned with the natural body axes), these matrices were computed based on previously obtained material properties.^{1,2} In this configuration, the bending-extension coupling coefficients, B_{ij} , the bending-twisting coefficients, D_{13} and D_{23} , and the shear-extension coupling coefficients, A_{13} and A_{23} , are all zero.

The material properties are 3.48 GPa for the elastic modulus, 517 MPa for the shear modulus, 0.137 for Poisson's ratio, and 657 kg m⁻³ for the mass density. Each ply is assumed to have a thickness of 2.54 mm.

Finite Element Analysis of GRSPMC Plates

Finite element models for GRSPMC laminated plates were developed based on the classical laminated plate theory. The models were generated using physical dimensions and the material properties mentioned above. MSC/NASTRAN was selected as the finite element code because of its multilayered composite element capabilities for normal mode analysis. The latter was achieved by using a real eigenvalue analysis that determines the natural frequencies and mode shapes of the plates with damping neglected. An updated finite element model is currently being developed so that damping can be incorporated into future research.

The equation of motion for natural frequencies and normal modes in the absence of damping and applied loading is

$$[M] \{\ddot{u}\} + [K] \{u\} = 0 \quad (2)$$

where $[M]$ is the mass matrix and $[K]$ is the stiffness matrix. The Lanczos method was used to extract the eigenvalues of the dynamic equations.

Each model consisted of quadrilateral isoparametric membrane-bending plate elements with uniform thickness. The finite element models were initially run with uniform element grids of 25.40 × 25.40 mm². Refinements in element sizes were made until the natural frequencies converged. The

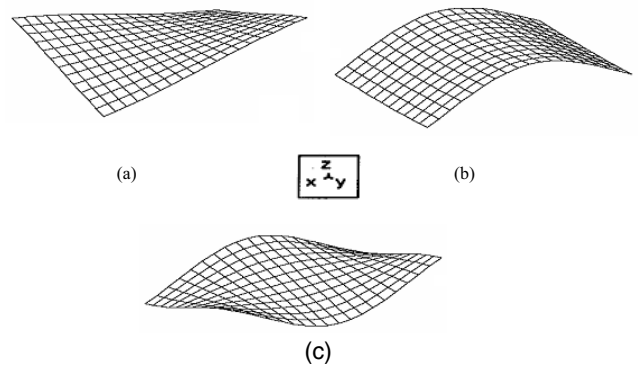


Fig. 1—Finite element mode shapes for a 152.40 × 228.60 mm² GRSPMC plate: (a) first mode, frequency = 269.50 Hz; (b) second mode, frequency = 410.86 Hz; (c) third mode, frequency = 674.20 Hz

resulting element mesh of 12.70 × 12.70 mm² was used for each of the models.

The composite properties were defined by considering the geometric properties of a 3-ply composite material laminate. The material properties were defined using an orthotropic material input for an isoparametric shell element. These data were developed from standardized material property testing as discussed earlier.¹

The pre- and post-processing of the finite element data were accomplished using MSC/PATRAN. The mode shapes and their corresponding natural frequencies were recovered, plotted, and animated in three dimensions to provide a visual understanding of the dynamic response for each plate.

Only the lower natural frequencies and mode shapes are of interest because they adequately describe the dynamic behavior of the laminate. Figure 1, for example, shows the first three mode shapes predicted for a 152.40 × 228.60 mm² GRSPMC plate; the corresponding natural frequencies are included in the figure caption.

Experimental Testing of GRSPMC Plates

Modal testing was conducted to validate the finite element models. Test plates were struck with an impact hammer attached to a load cell while suspended by elastic cords in a free-hanging configuration, and frequency response functions (FRFs) were measured over an array of points using an accelerometer.

Rigorously, an FRF is defined for a test article by developing a direct linear relationship between the mechanical force input and the measured response output. In our case, it is described by the formula

$$H(\omega) = \frac{Y(t)}{F_o e^{i\omega t}} \quad (3)$$

where $Y(t)$ is the acceleration measured in G, F_o is the input force, and $e^{i\omega t}$ is the exponential harmonic frequency function. Figure 2 shows a typical FRF plot taken from a plate at one of the measurement points.

Modal test data were collected using a Hewlett-Packard 3565 data acquisition system. The mode shapes and natural frequencies were determined with Leuven Measurement

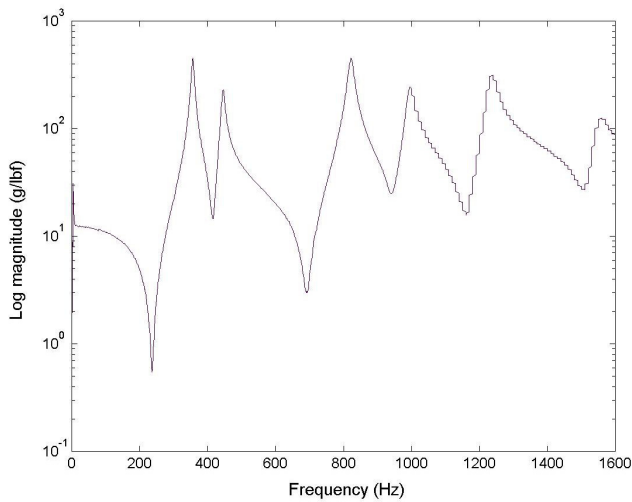


Fig. 2—Drive point FRF for a $152.40 \times 228.60 \text{ mm}^2$ GRSPMC plate

System (LMS) Cada-X software using the rational fraction polynomial method. The procedure is first to estimate how many modes there are in the bandwidth of interest, and then to estimate a pole for each mode. A residue is estimated for each mode. Mode shapes are curve fitted and computed based on these estimates using the software.

During the experiments, measurements were made in the transverse direction (z -axis) only, over a relatively coarse array. Since the focus of this investigation involved determining the first few lowest frequencies, a low spatial resolution corresponding to a minimum of nine measurement points on a plate was determined to be adequate.

Five $152.40 \times 228.60 \text{ mm}^2$ plates were initially tested to investigate how variations created during the fabrication process affected the dynamic characteristics. Table 2 shows the natural frequencies for the first three modes and their corresponding mean frequencies and standard deviations.

From statistical analysis, the intervals that contain 90% of the parent population for the frequencies with 90% confidence are 319.13–359.52 Hz, 393.74–452.73 Hz, and 758.37–831.61 Hz for the first, second, and third modes, respectively. It can be seen that all of the natural frequencies listed in Table 2 fall within these ranges, thereby illustrating that adequate control over the plate fabrication process exists.

Subsequent tests were performed on plates having aspect ratios from 0.5 to 4.5. Figure 3, for example, shows the first three mode shapes measured for a $152.40 \times 228.60 \text{ mm}^2$ GRSPMC plate; the corresponding natural frequencies are included in the figure caption.

The coherence transfer functions evaluated during the tests were close to 1.0 for most of the modes and the modes obtained after curve fitting all of the FRFs corresponded well with individual FRFs. The largest off-diagonal value in the cross modal assurance criterion (MAC) matrix was 0.2. Damping coefficients were approximately 1% for all of the plates tested and these values remained fairly consistent regardless of aspect ratio and frequency.

Discussion

In general, an agreement is observed between the experimental results and the finite element predictions, indicating

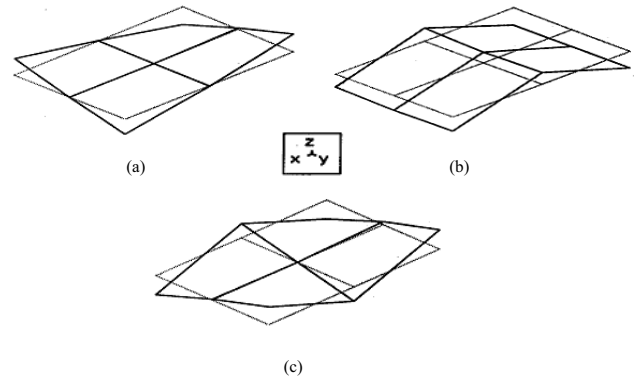


Fig. 3—Experimental mode shapes for a $152.40 \times 228.60 \text{ mm}^2$ GRSPMC plate: (a) first mode, frequency = 342.11 Hz; (b) second mode, frequency = 426.64 Hz; (c) third mode, frequency = 799.43 Hz

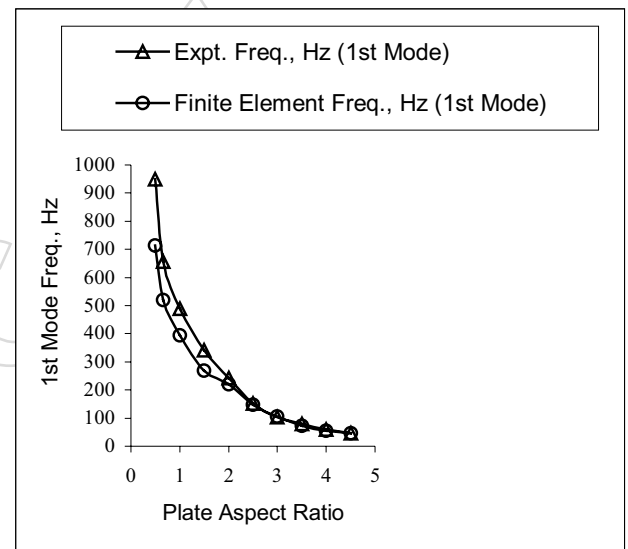


Fig. 4—Variation in the first mode experimental and finite element natural frequencies for free-free GRSPMC plates having various aspect ratios

that the material properties used in the finite element models are valid. This is evident, for example, for a $152.40 \times 228.60 \text{ mm}^2$ GRSPMC plate when the finite element predictions in Fig. 1 are compared to the test results in Fig. 3.

Figures 4, 5, and 6 show the test results and finite element predictions for the first three modes of all plates considered. The frequencies are highly dependent on the aspect ratios and decrease when the aspect ratio increases from 0.5 to 4.5. When the aspect ratio is greater than 4.5, the frequencies appear to taper off. These results are typical of specially orthotropic laminates and can be used to help predict the structural response, generate design data, and conduct parametric studies on large GRSPMC structures.

Tables 3, 4, and 5 show numerical comparisons between the experimental results and finite element predictions for the first three modes, respectively, of all plates considered. The mean absolute discrepancies between the frequencies

TABLE 2—FIRST THREE MODE NATURAL FREQUENCIES WITH THEIR MEAN AND STANDARD DEVIATION FREQUENCIES FOR FIVE, $152.40 \times 228.60 \text{ mm}^2$ PLATES

Mode	First Plate Frequency (Hz)	Second Plate Frequency (Hz)	Third Plate Frequency (Hz)	Fourth Plate Frequency (Hz)	Fifth Plate Frequency (Hz)	Mean Frequency (Hz)	Standard Deviation (Hz)
First mode	342.11	345.50	340.00	339.00	330.00	339.32	5.78
Second mode	426.64	432.50	426.00	421.00	410.00	423.23	8.44
Third mode	799.43	805.50	799.00	793.00	778.00	794.99	10.48

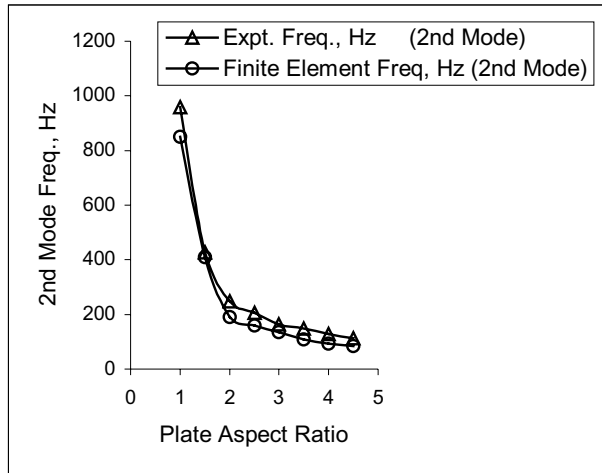


Fig. 5—Variation in the second mode experimental and finite element natural frequencies for free-free GRSPMC plates having various aspect ratios

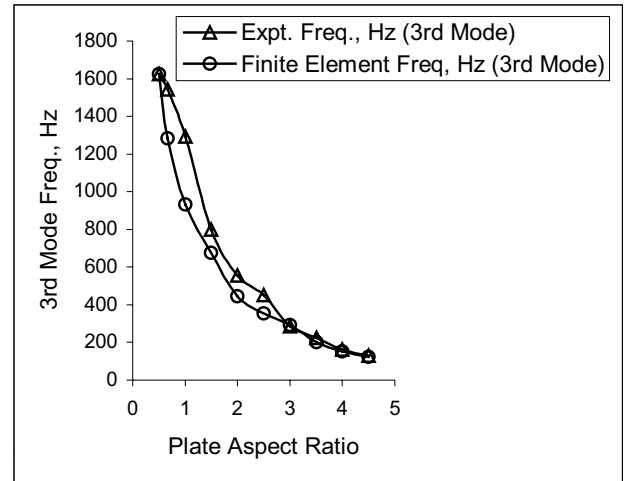


Fig. 6—Variation in the third mode experimental and finite element natural frequencies for free-free GRSPMC plates having various aspect ratios

are 11% for the first mode, 18% for the second mode, and 12% for the third mode. In all cases, the finite element analysis underpredicts the natural frequencies when compared to the experimental values. These discrepancies could be due to slight non-uniformities and rate dependence in the material properties, and variations in geometric dimensions of the plates.

Small discrepancies between the measured and calculated frequencies can be partially attributed to two problems in signal processing. The first is the noise present in the force or response signal as a result of a long time record. The second is the leakage present in the response signal as a result of a short time record.

Other reasons for frequency differences are that impact signals may be poorly suited for the FRF measurements, resolution bias errors may be present in the spectral estimates, and the system relating the output and input may not be linear. However, the main differences between the measured and calculated frequencies are most likely due to aberrations encountered while experimentally determining the material properties and the subsequent inaccuracies introduced into the constitutive equations used in the finite element models.

A frequency shift of approximately 3% was observed due to the mass loading of the 0.0017 kg accelerometer employed for testing. The smaller plates exhibited more deviations in the frequency shift than the larger plates due to their lower masses.

Another frequency shift was noted when additional tests were conducted two weeks after the initial tests were performed. The additional curing time and the hydration of the GRSPMC materials stiffened the plates and caused the frequencies to increase by approximately 3%.

Conclusions

An agreement between the experimental modal parameters and the finite element predictions indicates that standard impact modal testing can be applied to study GRSPMC materials. The accuracy of the finite element analysis shows that the finite element model based on the classical laminated plate theory is valid. Since GRSPMC materials behave like classical composite materials and the classical mechanics of composite material theory is applicable, it should be possible to predict the dynamic response of GRSPMC composite structures using the finite element model developed in this paper.

Acknowledgments

The authors would like to thank NASA, the U.S. Air Force, the U.S. Army, and the University of Alabama in Huntsville (UAH) for providing the facilities and resources that made this research possible. Thanks are also extended to the members of the American Society of Civil Engineering Student Chapter at UAH for formulating the GRSPMC mix design.

TABLE 3—COMPARISON BETWEEN THE EXPERIMENTAL AND THE FINITE ELEMENT FIRST (FUNDAMENTAL) MODE NATURAL FREQUENCIES FOR FREE–FREE GRSPMC PLATES HAVING VARIOUS ASPECT RATIOS

Plate Size (mm ²)	Thickness (mm)	Aspect Ratio	Experimental Frequency (Hz)	Finite Element Frequency (Hz)	% Difference
152.40 × 76.20	9.449	0.50	949.00	714.02	-24.76
152.40 × 101.06	8.941	0.67	657.12	520.36	-20.81
152.40 × 152.40	9.525	1.00	489.07	394.30	-19.38
152.40 × 228.60	9.677	1.50	342.11	269.50	-21.22
152.40 × 304.80	9.652	2.00	242.36	220.76	-8.91
152.40 × 381.00	10.109	2.50	152.38	148.38	-2.63
152.40 × 457.20	9.652	3.00	102.75	106.39	3.54
152.40 × 533.40	9.855	3.50	80.16	73.63	-8.15
152.40 × 609.60	9.754	4.00	59.34	55.96	-5.70
152.40 × 685.80	10.008	4.50	46.00	45.27	-1.59
				Mean % absolute discrepancy	11.67

TABLE 4—COMPARISON BETWEEN THE EXPERIMENTAL AND THE FINITE ELEMENT SECOND MODE NATURAL FREQUENCIES FOR FREE–FREE GRSPMC PLATES HAVING VARIOUS ASPECT RATIOS

Plate Size (mm ²)	Thickness (mm)	Aspect Ratio	Experimental Frequency (Hz)	Finite Element Frequency (Hz)	% Difference
152.40 × 76.20	9.449	0.50	1024.75	841.00	-17.93
152.40 × 101.60	8.941	0.67	861.62	794.17	-7.83
152.40 × 152.40	9.525	1.00	958.26	849.20	-11.38
152.40 × 228.60	9.677	1.50	426.64	410.86	-3.70
152.40 × 304.80	9.652	2.00	248.17	190.75	-23.14
152.40 × 381.00	10.109	2.50	205.28	158.52	-22.78
152.40 × 457.20	9.652	3.00	163.31	135.44	-17.07
152.40 × 533.40	9.855	3.50	148.11	108.65	-26.64
152.40 × 609.60	9.754	4.00	128.23	93.95	-26.73
152.40 × 685.80	10.008	4.50	113.00	85.15	-24.65
				Mean % absolute discrepancy	18.19

TABLE 5—COMPARISON BETWEEN THE EXPERIMENTAL AND THE FINITE ELEMENT THIRD MODE NATURAL FREQUENCIES FOR FREE–FREE GRSPMC PLATES HAVING VARIOUS ASPECT RATIOS

Plate Size (mm ²)	Thickness (mm)	Aspect Ratio	Experimental Frequency (Hz)	Finite Element Frequency (Hz)	% Difference
152.40 × 76.20	9.449	0.50	1623.80	1623.70	-0.01
152.40 × 101.60	8.941	0.67	1543.92	1284.40	-16.81
152.40 × 152.40	9.525	1.00	1292.66	933.05	-27.82
152.40 × 228.60	9.677	1.50	799.43	674.20	-15.66
152.40 × 304.80	9.652	2.00	556.76	443.54	-20.34
152.40 × 381.00	10.109	2.50	450.11	354.39	-21.27
152.40 × 457.20	9.652	3.00	287.08	291.88	1.67
152.40 × 533.40	9.855	3.50	223.41	202.25	-9.47
152.40 × 609.60	9.754	4.00	162.71	153.89	-5.42
152.40 × 685.80	10.008	4.50	130.00	124.55	-4.19
				Mean % absolute discrepancy	12.27

During that time, Dr. Houssam Toutanji and Dr. John Gilbert acted as the Chapter’s advisors. Portions of this work are included in the Proceedings of the 2003 SEM Annual Conference and Exposition on Experimental and Applied Mechanics, Charlotte, NC, June 2–4, Paper No. 133.

References

1. Vaughan, R.E. and Gilbert, J.A., “Analysis of Graphite Reinforced Ce-

mentitious Composites,” *Proceedings of the 2001 SEM Annual Conference and Exposition, Portland, OR, June 4–6, 532–535 (2001).*
 2. Biszick, K.R. and Gilbert, J.A., “Designing Thin-walled, Reinforced Concrete Panels for Reverse Bending,” *Proceedings of the 1999 SEM Spring Conference on Theoretical, Experimental and Computational Mechanics, Cincinnati, OH, June 7–9, 431–434 (1999).*
 3. Tsai, S.W. and Hahn, H.T., *Introduction to Composite Materials, Technomic Publishing, Lancaster, PA (1980).*
 4. Kollar, L.P. and Springer, G.S., *Mechanics of Composite Structures, Cambridge University Press, Cambridge (2003).*